Frontiers of Information Technology & Electronic Engineering
www.jzus.zju.edu.cn; engineering.cae.cn; www.springerlink.com
ISSN 2095-9184 (print); ISSN 2095-9230 (online)
E-mail: jzus@zju.edu.cn

Correspondence:

Low-cost high-order-mode cavity backed slot array antenna using empty substrate integrated waveguide for the 5G n260 band*

Zihang QI[1,2,3], Xiuping LI‡[1,2,3], Hua ZHU[1,2,3]

[1]*School of Electronic Engineering, Beijing University of Posts and Telecommunications, Beijing 100876, China*

[2]*Beijing Key Laboratory of Work Safety Intelligent Monitoring, Beijing 100876, China*

[3]*MOE Key Laboratory of Universal Wireless Communications, Beijing 100876, China*

E-mail: qizihang@bupt.edu.cn; xpli@bupt.edu.cn; judy-cool@163.com

Received Sept. 26, 2020; Revision accepted Jan. 25, 2021; Crosschecked Mar. 15, 2021

https://doi.org/10.1631/FITEE.2000503

1 Introduction

A low-cost slot array antenna is proposed for fifth-generation wireless communication (5G) n260 band applications. The antenna is based on the low-cost printed circuit board (PCB) material FR-4. Empty substrate-integrated waveguide is used to avoid high dielectric loss. High-order-mode cavities are introduced to reduce the complexity of the feeding network. The proposed antenna shows a maximum realized gain of 27 dBi with a radiation efficiency of 72.4%. The measurement and simulation results achieve good agreement. The proposed antenna can be a good candidate for low-cost millimeter-wave (mmWave) wireless communication systems.

Millimeter-wave antennas show great potential for future high-speed wireless communication. The Third Generation Partnership Project (3GPP) has defined the n260 band from 37 to 40 GHz for 5G new radio. Substrate-integrated waveguide (SIW) based antennas have been widely investigated (Chu et al., 2014; Li et al., 2017; Pasian et al., 2017) due to their advantages of low cost and high integration as compared with metal waveguide. Nevertheless, dielectric loss in SIW cannot be neglected in the mmWave regime. Low-loss materials are needed to achieve high efficiency, which will greatly increase the cost. Even so, dielectric loss is the main loss for SIW. To reduce the dielectric loss of SIW, the concept of a modified SIW using PCB with an air-cut region was proposed by Ranjkesh and Shahabadi (2006). Later on, empty SIW (ESIW), air-filled SIW (AFSIW), and hollow SIW (HSIW) were proposed and verified (Belenguer et al., 2014; Parment et al., 2014; Jin et al., 2014). The insertion loss for AFSIW is about 0.045 dB/cm, which is less than one third of that for the Rogers 6002-filled SIW at the Ka-band (Parment et al., 2015). Since then, researchers have provided phase shifters, filters, and antennas based on ESIW, AFSIW, and HSIW (Parment et al., 2016, 2017a, 2017b; Ghiotto et al., 2017).

Millimeter-wave antennas based on high-order-mode resonating cavities have been studied recently. Because one cavity can excite many slots at one time, a simple feeding network can be used in these designs. A single-fed slotted cavity antenna based on SIW technology using high-order cavity mode was demonstrated in Han et al. (2015). High-order resonate modes of TE_{130}, TE_{310}, and TE_{330} are excited by a

‡ Corresponding author

* Project supported by the National Key Research and Development Program of China (No. 2018YFF0212102), the National Natural Science Foundation of China (No. 61601050), and the Fundamental Research Funds for the Central Universities, China

ORCID: Zihang QI, https://orcid.org/0000-0002-5488-6404; Xiuping LI, https://orcid.org/0000-0003-4350-9651

coaxial probe. The antenna shows an impedance bandwidth of 26% (28–36.6 GHz). However, it is difficult to construct larger arrays using the coaxial probe. TE_{560} mode was employed in W-band SIW based 20×24 and 40×48 slot array antennas in Yuan et al. (2018). The measured peak gains are 26.39 dBi at 95.3 GHz and 30.36 dBi at 95.2 GHz. Nevertheless, the radiation efficiencies are 41.7% and 28.45%, respectively.

High-order-mode technology is quite important for ESIW antennas in mmWave bands because fabrication precision cannot be achieved in complicated high-density feeding networks. Furthermore, simplified feeding networks can reduce much insertion loss, resulting in high-gain and high-efficiency antennas.

In this correspondence, a low-cost high-order-mode slot array using ESIW is proposed for the 5G n260 band. TE_{340} mode cavities are introduced in the feeding network to excite 3×4 slots simultaneously. The feeding network is greatly simplified using high-order-mode cavities. The measurement results of the fabricated 12×16-slot array prototype are in good agreement with the simulation results.

2 Proposed antenna structure

2.1 3×4-slot subarray

The proposed 3×4-slot subarray is excited by an empty substrate integrated waveguide cavity (Fig. 1). TE_{340} mode can be excited in the cavity through a coupling slot on the third layer. Fig. 1b shows the E-field distribution at 38 GHz. Equal amplitude of the resonant nodes can be seen. The radiation slots are alternately placed at the right or left margin of the resonant nodes to excite them in the same phase.

The resonant frequency of the cavity can be calculated by

$$f_{mnp}=\frac{1}{2\pi\sqrt{\mu\varepsilon}}\sqrt{\left(\frac{m\pi}{a}\right)^2+\left(\frac{n\pi}{b}\right)^2+\left(\frac{p\pi}{c}\right)^2}, \quad (1)$$

where a, b, and c correspond to the width, length, and height of the cavity, respectively, and m, n, p indicate the numbers of variations in the standing wave pattern in the x, y, z directions, respectively. The dimensions of the subarray are given in Table 1.

Table 1 Parameters of the proposed slot array antenna (unit: mm)

a	b	c	dx	dy	p	s
23.3	17.2	4.7	7	5.73	2.83	4.7

Simulated S_{11} and the gain of the subarray are given in Fig. 2. The −10 dB impedance bandwidth covers 37–40 GHz. A maximum gain of 16.1 dBi is obtained at 38 GHz for the subarray. Radiation patterns on the E-plane and H-plane at 38 GHz are shown in Fig. 3. In this correspondence, simulation is performed using the Ansys High-Frequency Structure Simulator (HFSS). Metal loss is considered in the simulations except for the 2.4-mm connector.

2.2 12×16-slot array

To achieve a higher gain, a 12×16-slot array is designed based on the 3×4-slot subarray. An exploded view of the proposed slot array is shown in Fig. 4. The proposed 12×16-slot array is constructed with five PCB layers. The top layer is the radiation slots layer. The second layer is the high-order-mode resonant cavity layer. The third layer is the coupling layer which couples energy from the bottom feeding

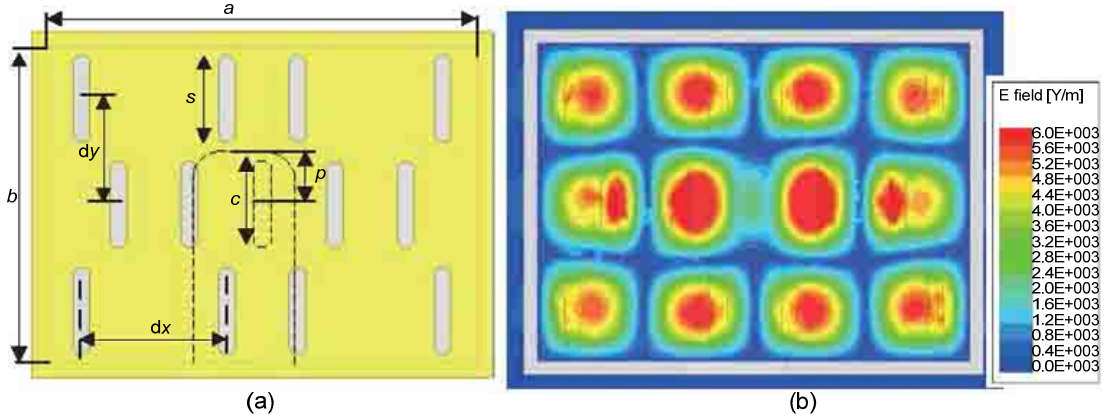

Fig. 1 The proposed 3×4 subarray: (a) dimensions of the subarray; (b) E-field distribution of the proposed subarray at 38 GHz

network. All of the layers use the FR-4 substrate with a relative permittivity of 4.4 and a loss tangent of 0.02. The thickness of the first, third, and bottom layers is h_1=0.4 mm. The thickness of layers 2 and 4 is h_2=1.6 mm. The total dimension of the slot array is 103.2 mm ×84.8 mm×4.4 mm. A 2.4-mm connector is used to feed the antenna. A simple transition is designed to convert TEM-wave into TE_{10}-wave. A two-way power divider is used in the feeding network (Fig. 5). Its simulated *S*-parameters are illustrated in Fig. 6. The impedance bandwidth can cover 36–41 GHz for $|S_{11}|$<−20 dB. Based on this two-way power divider, a 1–16 power divider is designed and used in the proposed 12×16-slot array.

3 Fabrication and measurement

The proposed antenna is fabricated layer by layer using low-cost PCB technology. Fig. 7 shows the top and bottom views of the fabricated antenna. The feeding network layer and high-order-mode cavity layer are also shown. Inner walls of these substrates are plated with about 30-μm-thick copper. Because there is no position for screws on the aperture, screws are located along all edges of the antenna and conductive adhesives are used in the center part to compress these PCB layers together.

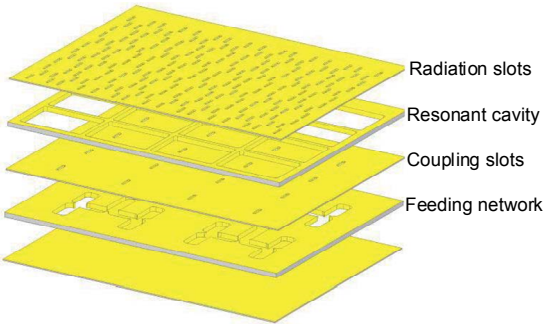

Fig. 4 Exploded view of the proposed slot array antenna

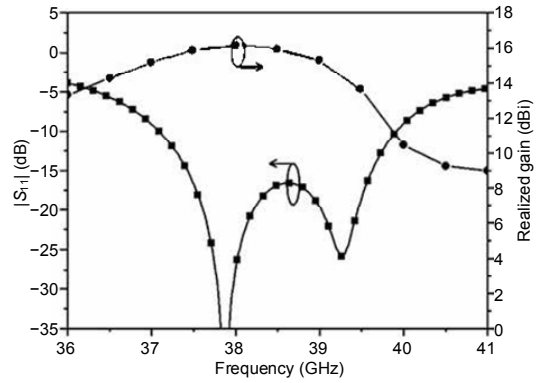

Fig. 2 Simulated $|S_{11}|$ and realized gain of the 3×4-slot subarray

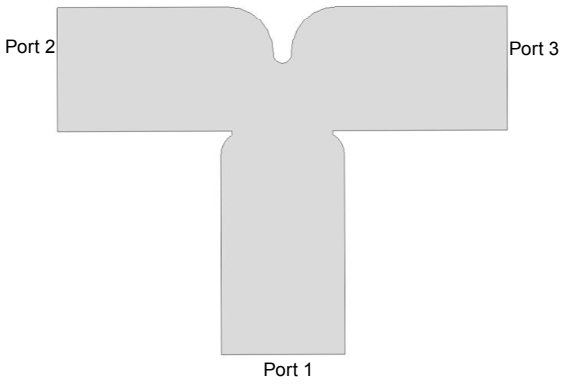

Fig. 5 Power divider structure

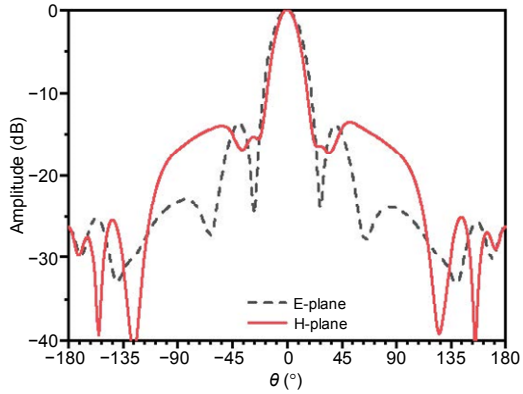

Fig. 3 Simulated radiation patterns at 38 GHz of the 3×4-slot subarray

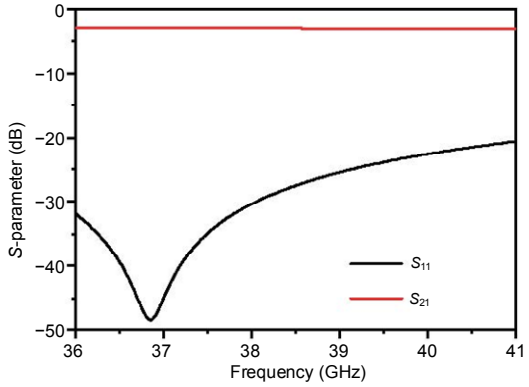

Fig. 6 Simulation results of the power divider in the feeding network

A 2.4-mm coaxial connector is used to feed the antenna. The impedance matching performance of the prototype is measured using a Keysight N5247A vector network analyzer. Radiation performance is measured in the far-field regime in an anechoic chamber. The measured $|S_{11}|$ in Fig. 8 shows some fluctuations compared with the simulated one. This may be due to the fabrication errors. The measured −8 dB impedance bandwidth of the prototype covers the n260 band. The measured maximum realized gain is 27 dBi, which is 1.3 dB lower than the simulated gain. By comparing the measured gain with the simulated directivity, the measured radiation efficiency of the slot array is estimated to be about 72.4%.

Fig. 9 compares the simulated and measured radiation patterns at 37, 38, 39, and 40 GHz. Measured co-polarized radiation patterns and simulated patterns

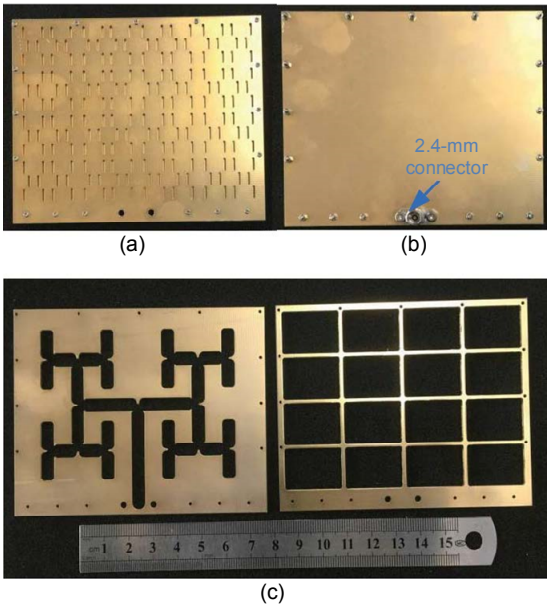

Fig. 7 Photographs of the fabricated slot array antenna: (a) top view of the assembled antenna; (b) bottom view of the assembled antenna; (c) feeding network layer and high-order-mode cavity layer

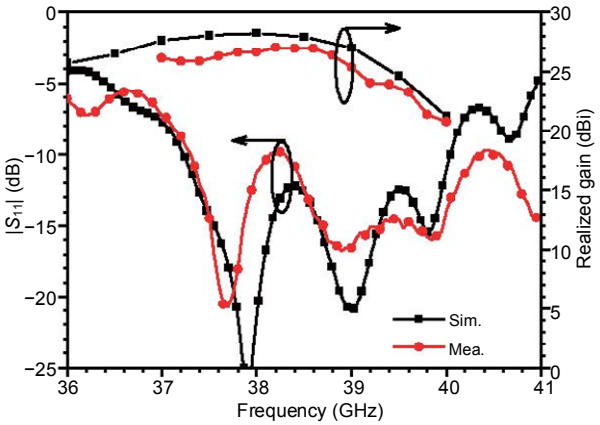

Fig. 8 Simulated and measured reflection coefficients and realized gains of the slot array antenna with a 2.4-mm connector

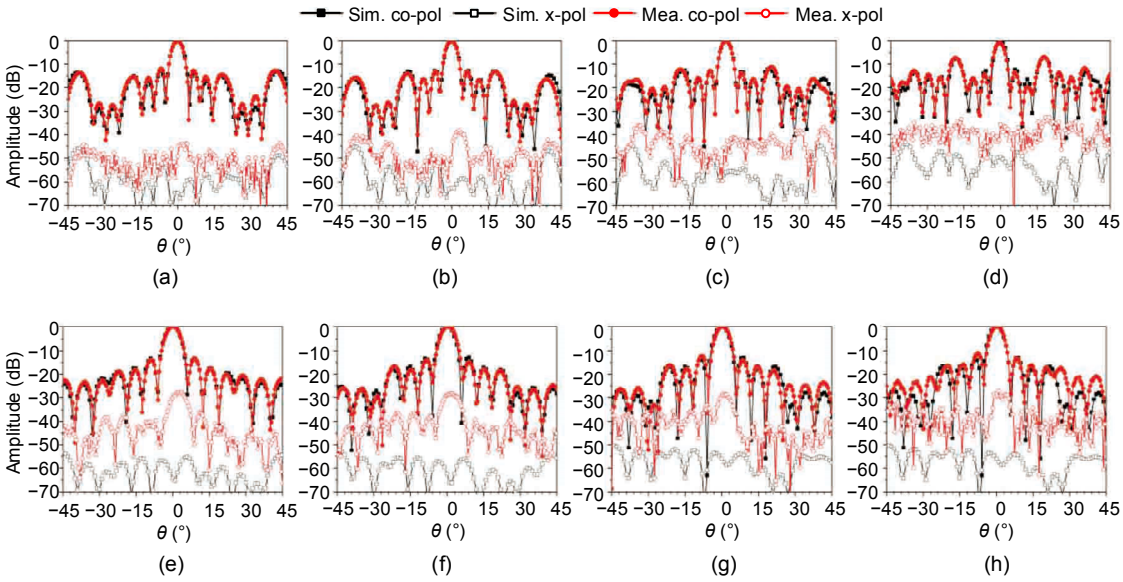

Fig. 9 Normalized radiation patterns of the slot array at 37 GHz for E-plane (a), 38 GHz for E-plane (b), 39 GHz for E-plane (c), 40 GHz for E-plane (d), 37 GHz for H-plane (e), 38 GHz for H-plane (f), 39 GHz for H-plane (g), and 40 GHz for H-plane (h)

show good agreement. However, some discrepancy can be seen for cross polarization. This may be due to some misalignment between the prototype antenna and the standard horn antenna. Because the distance between subarrays is larger than 1λ (λ is the free space wavelength), some grating lobes exist in the E-plane.

Table 2 compares the proposed antenna with other published slot array antennas. The proposed antenna shows a lower efficiency than the antenna of Qi et al. (2019). This is due to the air gaps between PCB layers, which result in energy leakage. Further adjustment can be made to improve the efficiency, such as using bonding film to avoid this leakage. As compared with SIW antennas, the proposed antenna has higher radiation efficiency and aperture efficiency.

4 Conclusions

In this correspondence we presented a low-cost, high-gain slot array antenna based on FR-4 PCB material for the 5G n260 band. The simplified feeding network implemented by high-order-mode cavities resulted in a high radiation efficiency. The performance was verified experimentally using a practical structure. Measurement results show good agreement with simulation results.

Contributors

Zihang QI designed the research and processed the data. Xiuping LI and Hua ZHU helped organize the manuscript. Zihang QI and Xiuping LI revised and finalized the paper.

Compliance with ethics guidelines

Zihang QI, Xiuping LI, and Hua ZHU declare that they have no conflict of interest.

References

Belenguer A, Esteban H, Boria VE, 2014. Novel empty substrate integrated waveguide for high-performance microwave integrated circuits. *IEEE Trans Microw Theory Techn*, 62(4):832-839. https://doi.org/10.1109/TMTT.2014.2309637

Chen XP, Wu K, Han L, et al., 2010. Low-cost high gain planar antenna array for 60-GHz band applications. *IEEE Trans Antenn Propag*, 58(6):2126-2129. https://doi.org/10.1109/TAP.2010.2046861

Chu P, Hong W, Wang KD, et al., 2014. Balanced substrate integrated waveguide filter. *IEEE Trans Microw Theory Techn*, 62(4):824-831. https://doi.org/10.1109/TMTT.2014.2307055

Ding Y, Wu K, 2009. A 4×4 ridge substrate integrated waveguide (RSIW) slot array antenna. *IEEE Antenn Wirel Propag Lett*, 8:561-564. https://doi.org/10.1109/LAWP.2009.2021006

Ghiotto A, Parment F, Vuong TP, et al., 2017. Millimeter-wave air-filled SIW antipodal linearly tapered slot antenna. *IEEE Antenn Wirel Propag Lett*, 16:768-771. https://doi.org/10.1109/LAWP.2016.2602280

Han WW, Yang F, Ouyang J, et al., 2015. Low-cost wideband and high-gain slotted cavity antenna using high-order modes for millimeter-wave application. *IEEE Trans Antenn Propag*, 63(11):4624-4631. https://doi.org/10.1109/TAP.2015.2473658

Jin LK, Lee RMA, Robertson I, 2014. Analysis and design of a novel low-loss hollow substrate integrated waveguide. *IEEE Trans Microw Theory Techn*, 62(8):1616-1624. https://doi.org/10.1109/TMTT.2014.2328555

Kim DY, Chung W, Park C, et al., 2011. Design of a 45°-inclined SIW resonant series slot array antenna for Ka-band. *IEEE Antenn Wirel Propag Lett*, 10:318-321. https://doi.org/10.1109/LAWP.2011.2141105

Li YJ, Wang JH, Luk KM, 2017. Millimeter-wave multibeam aperture-coupled magnetoelectric dipole array with planar substrate integrated beamforming network for 5G applications. *IEEE Trans Antenn Propag*, 65(12):6422-6431. https://doi.org/10.1109/TAP.2017.2681429

Liu B, Zhao RR, Ma Y, et al., 2018. A 45° linearly polarized slot array antenna with substrate integrated coaxial line technique. *IEEE Antenn Wirel Propag Lett*, 17(2):339-342. https://doi.org/10.1109/LAWP.2018.2789585

Parment F, Ghiotto A, Vuong TP, et al., 2014. Broadband transition from dielectric-filled to air-filled substrate integrated waveguide for low loss and high power handling millimeter-wave substrate integrated circuits. Proc IEEE

Table 2 Comparison between the proposed and reported slot arrays

Reference	Type	f_0 (GHz)	Scale	Gain (dBi)	Radiation efficiency	Aperture efficiency
Ding and Wu (2009)	RSIW	26	4×4	14.5	NA	26.3%
Chen et al. (2010)	SIW	60.6	12×12	22	68%	NA
Kim et al. (2011)	SIW	34.6	1×16	15.64	72.4%	21%
Liu et al. (2018)	SICL	34.5	5×6	17.09	NA	22%
Qi et al. (2019)	ESIW	38.7	8×6	24.0	86.5%	25.2%
This work	**ESIW**	**38.5**	**12×16**	**27**	**72.4%**	**27.7%**

RSIW: ridge substrate integrated waveguide; SICL: substrate integrated coaxial line. NA: not available

MTT-S Int Microwave Symp, p.1-3. https://doi.org/10.1109/MWSYM.2014.6848524

Parment F, Ghiotto A, Vuong TP, et al., 2015. Air-filled substrate integrated waveguide for low-loss and high power-handling millimeter-wave substrate integrated circuits. *IEEE Trans Microw Theory Techn*, 63(4):1228-1238. https://doi.org/10.1109/TMTT.2015.2408593

Parment F, Ghiotto A, Vuong TP, et al., 2016. Double dielectric slab-loaded air-filled SIW phase shifters for high-performance millimeter-wave integration. *IEEE Trans Microw Theory Techn*, 64(9):2833-2842. https://doi.org/10.1109/TMTT.2016.2590544

Parment F, Ghiotto A, Vuong TP, et al., 2017a. Ka-band compact and high-performance bandpass filter based on multilayer air-filled SIW. *Electron Lett*, 53(7):486-488. https://doi.org/10.1049/el.2016.4399

Parment F, Ghiotto A, Vuong TP, et al., 2017b. Millimetre-wave air-filled substrate integrated waveguide slot array antenna. *Electron Lett*, 53(11):704-706. https://doi.org/10.1049/el.2017.0102

Pasian M, Silvestri L, Rave C, et al., 2017. Substrate-integrated-waveguide E-plane 3-dB power-divider/combiner based on resistive layers. *IEEE Trans Microw Theory Techn*, 65(5):1498-1510. https://doi.org/10.1109/TMTT.2016.2642938

Qi ZH, Li XP, Xiao J, et al., 2019. Low-cost empty substrate integrated waveguide slot arrays for millimeter-wave applications. *IEEE Antenn Wirel Propag Lett*, 18(5):1021-1025. https://doi.org/10.1109/LAWP.2019.2907972

Ranjkesh N, Shahabadi M, 2006. Reduction of dielectric losses in substrate integrated waveguide. *Electron Lett*, 42(21):1230-1232. https://doi.org/10.1049/el:20061870

Yuan Q, Hao ZC, Fan KK, et al., 2018. A compact W-band substrate-integrated cavity array antenna using high-order resonating modes. *IEEE Trans Antenn Propag*, 66(12):7400-7405. https://doi.org/10.1109/TAP.2018.2871205